ACS Photonics

pubs.acs.org/journal/apchd5

Article

Optical All-Pass Filter Realized by Self-Compensation of Loss

Lu Xu,[#] Yuan Yu,[*,#] Xiaolong Liu, Xuewen Shu, and Xinliang Zhang[*]

Cite This: https://doi.org/10.1021/acsphotonics.1c00745

Read Online

ACCESS | Metrics & More | Article Recommendations | Supporting Information

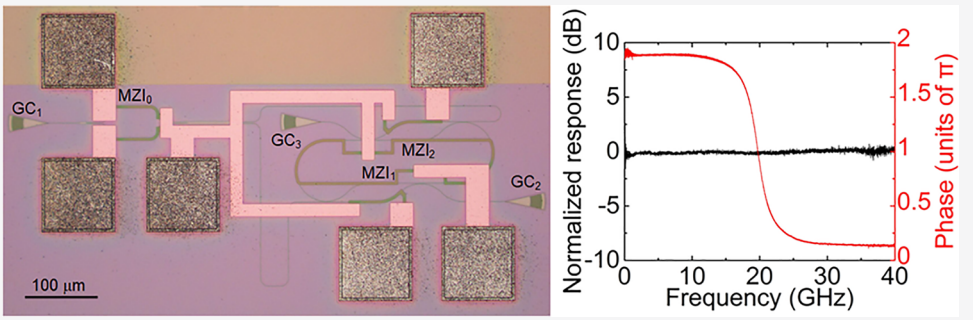

ABSTRACT: Filters are key devices in optical systems and are usually applied to signal suppression or selection based on their amplitude frequency responses. Different from amplitude filtering, an all-pass filter (APF) is a unique type of filter that exhibits a uniform amplitude and variable phase in the frequency response. Traditionally, an APF is designed to be ideal and waveguide loss as well as coupling loss are omitted, which is impossible in practice. Here we demonstrate a method of realizing an APF even when waveguide loss and coupling loss exist, and a feasible structure for realizing the APF with waveguide loss and coupling loss is proposed. The method indicates that an APF can be realized by introducing self-compensation of loss to the structure of an ideal single-stage APF, and further, an APF based on silicon-on-insulator foundry is fabricated and demonstrated. The method of self-compensation of loss can also be used to realize APFs in the electrical domain. We anticipate that our work will inspire realizations of more APF-related devices that once seemed impossible in practice, as well as loss related devices or structures.

KEYWORDS: *all-pass filter, silicon photonics, microwave photonics, microring resonator, microwave photonic phase shifter*

Filters have been widely used in signal processing systems to select desired signals and suppress interferences as well as noise based on their amplitude frequency responses.[1−5] Instead of manipulating power, an all-pass filter (APF) aims to manipulate the signal phase and exhibits a constant amplitude response with respect to frequency. In an APF, the phase response can be designed for different applications by utilizing suitable structures. With this unique characteristic, APFs are highly desired for occasions where only a phase variation is needed, such as the phase shifters,[6,7] dispersion compensation,[8−10] time delays,[11,12] ultrafast all-optical clock recovery,[13] and Hilbert transformers.[14,15]

General optical APF structures have been achieved in ideal lossless circumstances.[16] The research shows that in a lossless 2 × 2 network structure that consists of two inputs and two outputs, by connecting one output to one input with a delay line, the resulting structure is a single-stage APF. However, lossless transmission is impossible in practical waveguides, and the implementations of an APF in this manner are actually approximations of ideal APFs, but not real APFs.[9−12] The same problem also exists in the theoretical models[17−19] and fabricated devices[20−23] of electrical APFs.

To realize an APF, precise compensation of the transmission loss in the waveguide is of fundamental importance. In active waveguides, the transmission loss can be compensated by controlling and tailoring the gain spectrum in theory. However, it is rather difficult to precisely equalize the gain and loss, because the equalization is very sensitive to fluctuations in the input power and the injection current of the active waveguide. Therefore, to avoid lasing, the gain must be set to be lower than the loss, and consequently, the amplitude variations in the amplitude frequency response cannot be completely eliminated.

To resolve the challenge of precise loss compensation, here we propose to use optical interference between the through and drop ports of a silicon-based add-drop microring resonator (MRR). By adjusting the operating state, the device acts as if the transmission loss from the input to the through port is compensated. Hence, this approach can be called self-compensation of loss, in which the compensation is a power

Received: May 20, 2021

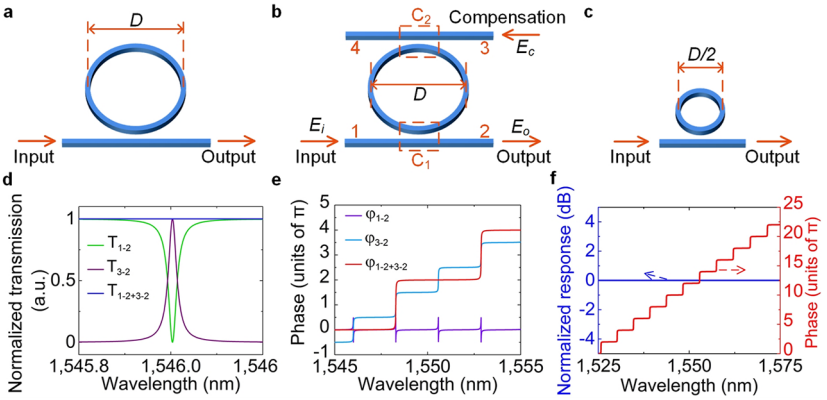

Figure 1. MRR-based APF. (a) The structure of a lossy all-pass MRR. The diameter of the MRR is represented by D. (b) The structure of the all-pass MRR with self-compensation of loss. The structure is the same as that of an add-drop MRR. Ports 1, 2, 3, and 4 represent the input, through, add, and drop ports of the add−drop MRR, respectively. C_1 and C_2 represent the two directional couplers connecting ports 1 with 2 and ports 3 with 4, respectively. (c) An ideal lossless all-pass MRR. The diameter of the MRR is $D/2$. The transmission spectra (d) and the phase responses (e) of the add−drop MRR when only the input (T_{1-2} and φ_{1-2}), only the compensation (T_{3-2} and φ_{3-2}), and the combined input and compensation ($T_{1-2+3-2}$ and $\varphi_{1-2+3-2}$) are injected into the device, respectively. (f) Simulated results of the MRR-based APF in (b).

scaling copy of the input. A feasible source for this kind of compensation is to take a slice from the input. When the compensation precisely equals the transmission loss, an APF can then be realized.

PRINCIPLE

Here, we consider an all-pass MRR, which exhibits all-pass transmission only for lossless transmission (see section 1 in the Supporting Information), as an example to demonstrate the method we proposed. A detailed demonstration of the realization of a general single-stage APF by using self-compensation of loss is given in section 1 of the Supporting Information. Here the APF is realized without omitting the waveguide loss and coupling loss. It is referred to as lossy APF in the following part for convenience. The transfer function of a lossy all-pass MRR (Figure 1a) can be expressed as

$$H = \frac{r_1 - ae^{i\varphi}}{1 - r_1 ae^{i\varphi}} \tag{1}$$

where r_1 is the self-coupling coefficient, φ is the round-trip phase shift of the MRR, and a is the round-trip amplitude transmission, including both the propagation loss in the MRR and the coupling loss in the coupler[24] (the influence of the coupling loss on transmission of the APF is discussed separately in section 2 in the Supporting Information). Here, $a = \exp(-\alpha L/2)$, where α is the power attenuation coefficient and L is the perimeter of the MRR. We can conclude that $a = 1$ for lossless transmission. Based on the structure of an all-pass MRR, the self-compensation can be implemented by adding another straight waveguide to be coupled with the MRR. The resulted structure of the APF (Figure 1b) is the same as that of a typical add−drop MRR, and the compensation is injected into the MRR via the add port (port 3 in Figure 1b). It should be stressed that the phase of the compensation is the same as that of the input.

To realize the APF, two conditions must be satisfied (see section 1 in the Supporting Information). Here, in the case of a MRR-based APF, condition 1 is that the add−drop MRR is critically coupled[24] for the input at port 1, indicating that $r_1 = r_2 a$, where r_1 and r_2 are the self-coupling coefficients of couplers C_1 and C_2 (Figure 1b), respectively. Assume that the amplitudes of the input at port 1 and the compensation at port 3 are represented by E_i and E_c, respectively. Condition 2 is that the amplitude ratio between E_c and E_i, which is represented by x, satisfies $x = k_1/(k_2\sqrt{a})$ (see section 1 in the Supporting Information), where k_1 and k_2 are the cross-coupling coefficients of couplers C_1 and C_2 (Figure 1b), respectively. Under the two conditions, when the input and the compensation are injected into the MRR alternatively, the corresponding transmission spectra from port 1 to port 2 and from port 3 to port 2 are shown by the green and purple curves in Figure 1d, respectively. It can be observed that the two transmission spectra are complementary to each other. However, when the two conditions are satisfied and the input and compensation are injected into the MRR simultaneously, the transfer function of the add−drop MRR from port 1 to port 2 is calculated to be (see section 2 in the Supporting Information)

$$H = \frac{E_o}{E_i} = \frac{r_1 - e^{i(\varphi/2)}}{1 - r_1 e^{i(\varphi/2)}} \tag{2}$$

where E_o represents the amplitude of the output at port 2 (Figure 1b). By comparing eq 1 and eq 2, we can observe that the add−drop MRR is equivalent to a lossless all-pass MRR, which is an ideal APF. From eq 2 it can be calculated that the transfer function satisfies $|H|^2 = 1$, shown as the blue curve in Figure 1d. This is in accordance with the definition of an APF. The corresponding phase responses (Figure 1e) show that, when both the input and the compensation are injected into the add−drop MRR simultaneously, the free spectral range (FSR) of the phase response (red curve in Figure 1e) is twice the FSR of the phase response when only the input or the compensation is injected into the MRR, indicating that the round-trip phase shift of the equivalent lossless all-pass MRR is $\varphi/2$. Consequently, under the two conditions, the lossy add−drop MRR after loss compensation is equivalent to the ideal lossless APF shown in Figure 1c. Here, both the waveguide loss and coupling loss in the APF shown in Figure 1c are omitted and the achieved APF is referred to as lossless APF in the following part for convenience. In the equivalent ideal lossless APF, the self-coupling and cross-coupling coefficients are r_1 and k_1, respectively, and the perimeter is one-half that of the

https://doi.org/10.1021/acsphotonics.1c00745
ACS Photonics XXXX, XXX, XXX−XXX

lossy add−drop MRR (Figure 1b). Figure 1f shows the simulated response of the lossy add−drop MRR when the optical signal is transmitted from port 1 to port 2 after self-compensation of loss, which is equivalent to that of the ideal lossless all-pass MRR (Figure 1c). In Figure 1f, we can observe that the amplitude response is constant with respect to wavelength in a wide wavelength range, while the phase varies periodically. Condition 1 determines the coupling ratios of the MRR, while condition 2 determines the power splitting ratio between the input and the compensation. These two conditions must be satisfied simultaneously to ensure the wide-range all-pass transmission. Therefore, the combined result of conditions 1 and 2 is that the transmission of the input in the MRR is exactly compensated by the method of self-compensation of loss and a real APF can be achieved.

RESULTS

To eliminate the influence of fabrication error on the deviations of the coupling coefficients, we propose a Mach−Zehnder interferometer (MZI)-assisted MRR structure (Figure 2a) to realize the APF. In this structure, the MZIs are designed to achieve the desired coupling coefficients with controllable adjustments.[25] MZI_1 and MZI_2 each have two directional couplers and the self-coupling and cross-coupling coefficients of the couplers are both r_1 and k_1 in MZI_1 and are both r_2 and k_2 in MZI_2, respectively. In Figure 2a,b, the centers of the couplers are marked with orange dots and represented by capital letters. Then, the waveguides can be marked by capital letters at the terminals of the waveguides. The lengths of the waveguides AC, BD, EG, and FH are all L_1, and their amplitude transmission a_1 satisfies $a_1 = \exp(-\alpha L_1/2)$. Similarly, the lengths of the delay lines DE and GB are both L_0, and their amplitude transmission a_0 satisfies $a_0 = \exp(-\alpha L_0/2)$. φ_0 is the phase shift of the delay lines DE and GB, φ_1 is the phase shift of AC, BD, and EG, and φ_2 is the phase shift of FH. According to conditions 1 and 2, it can be demonstrated that the structure in Figure 2a is an APF when the parameters satisfy the following (see section 3 in the Supporting Information):

$$r_2 = \sqrt{\frac{r_1^2 - k_1^2 + y a_0^2 a_1^2}{(y+1)a_0^2 a_1^2}}$$

$$x = \frac{2k_1 r_1}{(y+1)k_2 r_2 a_0 a_1} \tag{3}$$

where $y = \exp[i(\varphi_2 - \varphi_1)]$ and $x = E_c/E_i$. Figure 2b shows the structure of an ideal lossless APF based on an MZI (see section 3 in the Supporting Information). The phase shifts of A′C′ and B′D′ are both φ_1, which is the same as the phase shifts of AC and BD. The phase shift of D′I′B′ is the same as that of DE or GB and equal to φ_0. The waveguides in Figure 2b are all lossless. It can be demonstrated that the MZI-assisted MRR in Figure 2a is equivalent to the ideal lossless APF in Figure 2b (see section 3 in the Supporting Information).

According to the theoretical analysis, the structure shown in Figure 2c can be designed to realize an APF based on the MZI-assisted MRR by using self-compensation of loss. The optical signal is input into the photonic chip via a grating coupler (GC_1 in Figure 2c) and equally split into the two arms of MZI_0 by a 1 × 2 multimode interferometer (MMI).[26] MZI_0 is then connected with a 2 × 2 MMI, and the power splitting ratio between the two outputs can be adjusted by changing the

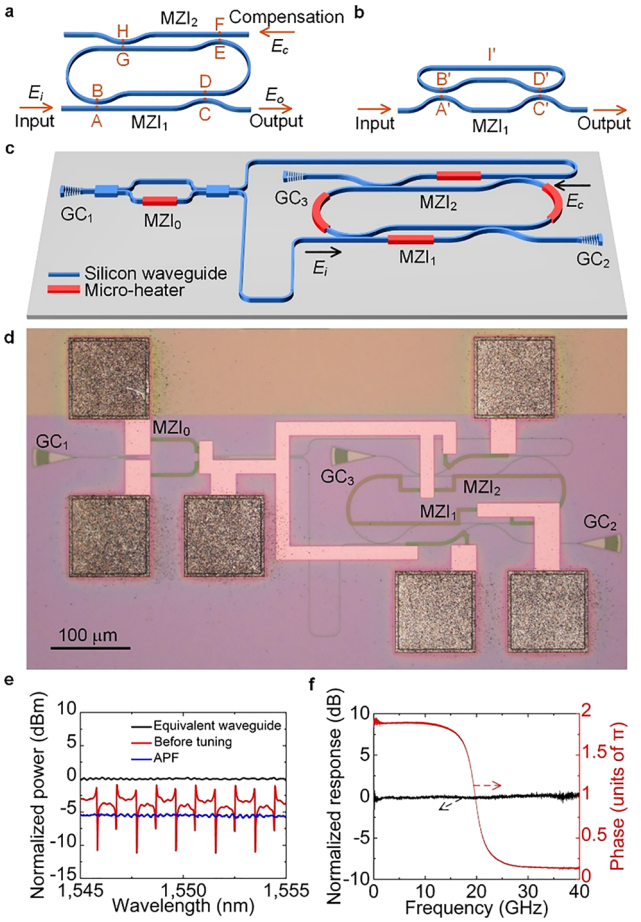

Figure 2. Realization of an APF based on the MZI-assisted MRR. (a) The structure of the MZI-assisted MRR. (b) The structure of an ideal lossless APF based on an MZI. (c) The structure of the designed APF. (d) A micrograph of the fabricated APF based on SOI foundry. Here, a spare microheater is added to the upper arm of MZI_0. (e) Measured optical transmission spectra of the fabricated device. The blue curve shows the measured optical spectrum of the fabricated APF, the red curve shows the measured optical spectrum of the device when no voltages are applied to the microheaters, and the black curve shows the transmission of the equivalent optical waveguide. (f) Amplitude and phase frequency responses of the proposed APF measured by a vector network analyzer (VNA).

phase difference between the two arms of MZI_0[27] via a microheater deposited on the lower arms of MZI_0. After MZI_0, the optical signal at the lower port acts as the input E_i, and the optical signal at the upper port acts as the compensation E_c. Then, two waveguides of the same length (ensuring that no phase difference exists between the input and compensation) are used to deliver the input and compensation to the MRR, respectively. Based on the designed lossy APF shown in Figure 2c, the fabricated APF based on silicon-on-insulator (SOI) foundry is shown in Figure 2d.

In the structure shown in Figure 2c, conditions 1 and 2 can be satisfied by adjusting the voltages applied to the microheaters of MZI_0, MZI_1, and MZI_2. When the two conditions are not satisfied simultaneously, the optical power transmission from GC_1 to GC_2 varies periodically with respect to wavelength (red curve in Figure 2e). By adjusting the voltages applied to the microheaters to satisfy conditions 1 and 2, the power transmission spectrum at the output of the APF is shown by the blue curve in Figure 2e. Compared with the red

https://doi.org/10.1021/acsphotonics.1c00745
ACS Photonics XXXX, XXX, XXX−XXX

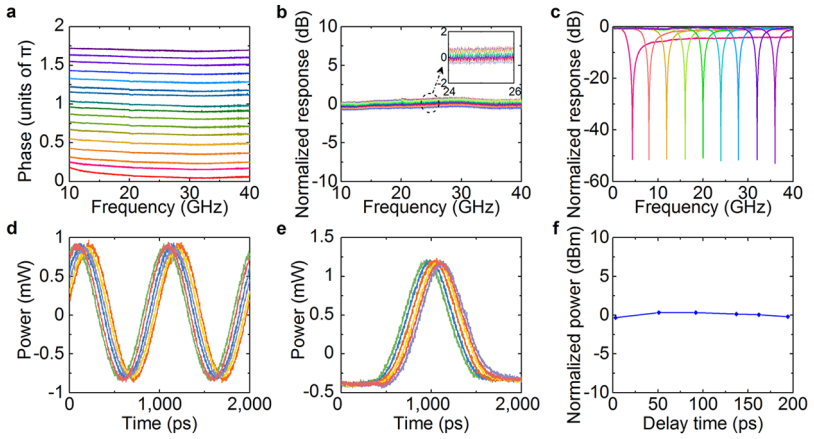

Figure 3. Results of possible applications based on the fabricated APF. Phase (a) and amplitude (b) frequency responses with different phase shifts when the APF works as a microwave photonic phase shifter. (c) The microwave photonic notch filter based on the APF with different central frequencies. Different measured time delays of the APF when the input is a sinusoidal signal with a frequency of 1 GHz (d) and a Gaussian pulse with a bandwidth of 500 ps and a repetition rate of 500 MHz (e). (f) The normalized output optical power for different time delays.

curve, we can observe that the periodic power variations at the resonance wavelengths no longer exist. We also compare the measured transmission spectrum of the APF with that of an equivalent single-mode waveguide (see section 4 in the Supporting Information) shown as the black curve in Figure 2e. We can observe that the transmission spectrum of the APF is in good agreement with that of the equivalent optical waveguide, except for an extra transmission loss of approximately 5 dB, which is caused by the compensation used for self-compensation of loss. In the APF operation, one part of the input optical signal is split into the upper waveguide by MZI_0 and used as the compensation. Therefore, extra transmission loss is generated. Slight ripples of blue and black curves with a maximal amplitude of approximately 0.3 dB and an FSR of approximately 0.3 nm are generated by the Fabry-Pérot cavities formed by GC_1 and GC_2 as well as by GC_1 and GC_3, simultaneously. These ripples can be reduced by further optimizing the grating couplers. To measure the amplitude and phase frequency responses precisely, the fabricated APF is also measured by a vector network analyzer (VNA; see section 5 in the Supporting Information), and the results are shown in Figure 2f. We can observe that the amplitude remains constant, while the phase has a variation of 1.8π within 40 GHz. It can be observed that the frequency range of the demonstrated APF covers 10 FSRs with no obvious power variation. Strictly speaking, the coupling coefficient and the phase shift induced by the microheater are frequency relevant. They are the ultimate limits that determine the limitation of the frequency range of the demonstrated APF. Therefore, we can conclude that the APF is successfully realized. It should be noted that all-pass transmission can alternatively be achieved via GC_3 when the microheaters are adjusted correspondingly to satisfy the two conditions for the optical transmission from GC_1 to GC_3.

Since only phase variations exist in the frequency response of the APF and the amplitude remains constant, some interesting applications can be explored based on the fabricated APF (the experimental details are shown in section 5 in the Supporting Information). The APF is an ideal device for a microwave photonic phase shifter. By adjusting the voltage applied to the microheaters deposited on the MRR, the measured microwave phase shifts and the corresponding amplitudes with respect to frequency are shown in Figure 3a and b, respectively. In Figure 3b, it can be observed that there is a power variation of approximately 0.4 dB in every amplitude frequency response curve, which is generated by the transmission ripples caused by the Fabry-Pérot effect (Figure 2e). During the adjustment of the microwave phase shift, we can see that the output microwave power changes slightly and the power variation is less than 0.8 dB. This is caused by thermal crosstalk during the adjustment of the microheater on the MRR, which can be reduced by using thermal isolation trenches.[28] Compared with conventional phase shifters,[29] it can realize adjustable phase shifts with relatively low power variation and no more adjustments of the MZIs are needed during the phase adjusting process, which simplified the operation of the whole system.

Based on the optical phase shifter, a single notch microwave photonic filter is also realized (Figure 3c). The rejection ratio is over 50 dB, and the central frequency can be tuned from 0 to 40 GHz, which is limited by the bandwidth of the modulator. Based on the proposed APF, tunable time delays can also be achieved with almost invariant output power. A sinusoidal signal and a Gaussian pulse are used in the experiment to measure the time delay, respectively. The measured maximum time delays of both the sinusoidal signal and Gaussian pulse are approximately 200 ps (Figure 3d and Figure 3e). When the time delay is changed by adjusting the voltage applied to the microheater on the MRR, the measured power variation of the optical signal is less than 0.4 dB (Figure 3f).

CONCLUSIONS

In conclusion, by using self-compensation of loss, we have demonstrated a real APF based on an add-drop MRR even when transmission loss exists, and an APF based on an MZI-assisted MRR has been demonstrated and fabricated using the SOI foundry. Applications of the proposed APF in a microwave phase shifter, a microwave photonic filter, and time delays have been explored. We believe that the method of self-compensation of loss employed for realizing the APF holds great potential in numerous fields of research. Our work opens up a possible path for realizing devices that seemed to be impossible in the past, such as amplitude distortion-free Hilbert transformers[15,30,31] and microwave photonic phase shifters. With fabrication improvements in the future, the

https://doi.org/10.1021/acsphotonics.1c00745
ACS Photonics XXXX, XXX, XXX−XXX

realization of an APF will be simplified, and more efforts should be devoted to exploring the potential of APFs.

■ ASSOCIATED CONTENT

Supporting Information

The Supporting Information is available free of charge at https://pubs.acs.org/doi/10.1021/acsphotonics.1c00745.

Demonstration of the general single-stage APF; demonstration of the APF based on the add−drop MRR; demonstration of the APF based on a MZI-assisted MRR; adjusting the fabricated device to function as an equivalent optical waveguide; device fabrication and experimental details (PDF)

■ AUTHOR INFORMATION

Corresponding Authors

Yuan Yu − *Wuhan National Laboratory for Optoelectronics, Huazhong University of Science and Technology, Wuhan, Hubei 430074, People's Republic of China; School of Optical and Electronic Information, Huazhong University of Science and Technology, Wuhan, Hubei 430074, People's Republic of China;* orcid.org/0000-0001-7400-5064; Email: yuan_yu@hust.edu.cn

Xinliang Zhang − *Wuhan National Laboratory for Optoelectronics, Huazhong University of Science and Technology, Wuhan, Hubei 430074, People's Republic of China; School of Optical and Electronic Information, Huazhong University of Science and Technology, Wuhan, Hubei 430074, People's Republic of China*; Email: xlzhang@mail.hust.edu.cn

Authors

Lu Xu − *Wuhan National Laboratory for Optoelectronics, Huazhong University of Science and Technology, Wuhan, Hubei 430074, People's Republic of China; School of Optical and Electronic Information, Huazhong University of Science and Technology, Wuhan, Hubei 430074, People's Republic of China; National Information Optoelectronics Innovation Center, China Information and Communication Technologies Group Corporation, Wuhan, Hubei 430074, People's Republic of China*

Xiaolong Liu − *Wuhan National Laboratory for Optoelectronics, Huazhong University of Science and Technology, Wuhan, Hubei 430074, People's Republic of China; School of Optical and Electronic Information, Huazhong University of Science and Technology, Wuhan, Hubei 430074, People's Republic of China*

Xuewen Shu − *Wuhan National Laboratory for Optoelectronics, Huazhong University of Science and Technology, Wuhan, Hubei 430074, People's Republic of China;* orcid.org/0000-0003-4888-0767

Complete contact information is available at: https://pubs.acs.org/10.1021/acsphotonics.1c00745

Author Contributions

#L.X. and Y.Y. contributed equally to this work. L.X., Y.Y., and X.L. conceived the idea. L.X. and Y.Y. performed the numerical simulations and constructed the theoretical framework. L.X., Y.Y., and X.L. designed and fabricated the devices. L.X. and Y.Y. performed the measurements and prepared the paper. All the authors discussed the results and edited the manuscript. Y.Y., X.S., and X.Z. supervised the project.

Notes

The authors declare no competing financial interest.

■ ACKNOWLEDGMENTS

This work was supported by the National Key R&D Program of China (2018YFB2201700, 2018YFA0704403), the National Natural Science Foundation of China (61975249), the Program for HUST Academic Frontier Youth Team (2018QYTD08).

■ REFERENCES

(1) Magden, E. S.; Li, N.; Raval, M.; Poulton, C. V.; Ruocco, A.; Singh, N.; Vermeulen, D.; Ippen, E. P.; Kolodziejski, L. A.; Watts, M. R. Transmissive silicon photonic dichroic filters with spectrally selective waveguides. *Nat. Commun.* **2018**, *9*, 1−10.

(2) Sancho, J.; Bourderionnet, J.; Lloret, J.; Combrié, S.; Gasulla, I.; Xavier, S.; Sales, S.; Colman, P.; Lehoucq, G.; Dolfi, D.; Capmany, J.; Rossi, A. D. Integrable microwave filter based on a photonic crystal delay line. *Nat. Commun.* **2012**, *3*, 1−9.

(3) Fandiño, J. S.; Muñoz, P.; Doménech, D.; Capmany, J. A monolithic integrated photonic microwave filter. *Nat. Photonics* **2017**, *11*, 124−129.

(4) Supradeepa, V. R.; Long, C. M.; Wu, R.; Ferdous, F.; Hamidi, E.; Leaird, D. E.; Weiner, A. M. Comb-based radiofrequency photonic filters with rapid tunability and high selectivity. *Nat. Photonics* **2012**, *6*, 186−194.

(5) Zhuang, L.; Roeloffzen, C. G. H.; Hoekman, M.; Boller, K.-J.; Lowery, A. J. Programmable photonic signal processor chip for radiofrequency applications. *Optica* **2015**, *2*, 854−859.

(6) Adams, D. B.; Madsen, C. K. A novel broadband photonic RF phase shifter. *J. Lightwave Technol.* **2008**, *26*, 2712−2717.

(7) Yang, W.; Sun, T.; Rao, Y.; Megens, M.; Chan, T.; Yoo, B.-W.; Horsley, D. A.; Wu, M. C.; Chang-Hasnain, C. J. High speed optical phased array using high contrast grating all-pass filters. *Opt. Express* **2014**, *22*, 20038−20044.

(8) Madsen, C. K.; Lenz, G. Optical all-pass filters for phase response design with applications for dispersion compensation. *IEEE Photonics Technol. Lett.* **1998**, *10*, 994−996.

(9) Jablonski, M.; Takushima, Y.; Kikuchi, K. The realization of all-pass filters for third-order dispersion compensation in ultrafast optical fiber transmission systems. *J. Lightwave Technol.* **2001**, *19*, 1194−1205.

(10) Lunardi, L. M.; Moss, D. J.; Chandrasekhar, S.; Buhl, L. L.; Lamont, M.; McLaughlin, S.; Randall, G.; Colbourne, P.; Kiran, S.; Hulse, C. A. Tunable dispersion compensation at 40-Gb/s using a multicavity Etalon all-pass filter with NRZ, RZ, and CS-RZ modulation. *J. Lightwave Technol.* **2002**, *20*, 2136−2144.

(11) Madsen, C. K. Subband all-pass filter architectures with applications to dispersion and dispersion-slope compensation and continuously variable delay lines. *J. Lightwave Technol.* **2003**, *21*, 2412−2420.

(12) Kim, J.; Ko, Y.; Kim, H.; Chung, Y. Variable time delay experiments in serially cascaded ring resonator all-pass filters. *18th OptoElectronics and Commun. Conf. held jointly with 2013 International Conf. on Photonics in Switching*, Kyoto, Japan, 30 Jun - 05 Jul 2013, Optica, 2013.

(13) Maram, R.; Kong, D.; Galili, M.; Oxenløwe, L. K.; Azaña, J. Ultrafast all-optical clock recovery based on phase-only linear optical filtering. *Opt. Lett.* **2014**, *39*, 2815−2818.

(14) Zhuang, L.; Khan, M. R.; Beeker, W.; Leinse, A.; Heideman, R.; Roeloffzen, C. Novel microwave photonic fractional Hilbert transformer using a ring resonator-based optical all-pass filter. *Opt. Express* **2012**, *20*, 26499−26510.

(15) Liu, W.; Li, M.; Guzzon, R. S.; Norberg, E. J.; Parker, J. S.; Lu, M.; Coldren, L. A.; Yao, J. A fully reconfigurable photonic integrated signal processor. *Nat. Photonics* **2016**, *10*, 190−195.

(16) Lenz, G.; Madsen, C. K. General optical all-pass filter structures for dispersion control in WDM systems. *J. Lightwave Technol.* **1999**, *17*, 1248−1254.
(17) Ibrahim, M. A.; Kuntman, H.; Cicekoglu, O. First-order all-pass filter canonical in the number of resistors and capacitors employing a single DDCC. *Circuits, Syst. Signal Process.* **2003**, *22*, 525−536.
(18) Minaei, S.; Yuce, E. Novel voltage-mode all-pass filter based on using DVCCs. *Circuits, Syst. Signal Process.* **2010**, *29*, 391−402.
(19) Minaei, S.; Cicekoglu, O. A resistorless realization of the first-order all-pass filter. *Int. J. Electron.* **2006**, *93*, 177−183.
(20) Gupta, S.; Zhang, Q.; Zou, L.; Jiang, L. J.; Caloz, C. Generalized coupled-line all-pass phasers. *IEEE Trans. Microwave Theory Tech.* **2015**, *63*, 1007−1018.
(21) Guyette, A. C.; Naglich, E. J.; Shin, S. Switched allpass-to-bandstop absorptive filters with constant group delay. *IEEE Trans. Microwave Theory Tech.* **2016**, *64*, 2590−2595.
(22) Naglich, E. J.; Lee, J.; Peroulis, D.; Chappell, W. J. Switchless tunable bandstop-to-all-pass reconfigurable filter. *IEEE Trans. Microwave Theory Tech.* **2012**, *60*, 1258−1265.
(23) Viveiros, D.; Consonni, D.; Jastrzebski, A. K. A tunable all-pass MMIC active phase shifter. *IEEE Trans. Microwave Theory Tech.* **2002**, *50*, 1885−1889.
(24) Bogaerts, W.; De Heyn, P.; Van Vaerenbergh, T.; De Vos, K.; Kumar Selvaraja, S.; Claes, T.; Dumon, P.; Bienstman, P.; Van Thourhout, D.; Baets, R. Silicon microring resonators. *Laser Photonics Rev.* **2012**, *6*, 47−73.
(25) Zhou, L.; Poon, A. W. Electrically reconfigurable silicon microring resonator-based filter with waveguide-coupled feedback. *Opt. Express* **2007**, *15*, 9194−9204.
(26) Thomson, D. J.; Hu, Y.; Reed, G. T.; Fedeli, J. Low loss MMI couplers for high performance MZI modulators. *IEEE Photonics Technol. Lett.* **2010**, *22*, 1485−1487.
(27) Feng, D. J. Y.; Lay, T. S. Compact multimode interference couplers with arbitrary power splitting ratio. *Opt. Express* **2008**, *16*, 7175−7180.
(28) Dong, P.; Qian, W.; Liang, H.; Shafiiha, R.; Feng, D.; Li, G.; Cunningham, J. E.; Krishnamoorthy, A. V.; Asghari, M. Thermally tunable silicon racetrack resonators with ultralow tuning power. *Opt. Express* **2010**, *18*, 20298−20304.
(29) Chew, S. X.; Huang, D.; Li, L.; Song, S.; Tran, M. A.; Yi, X.; Bowers, J. E. Integrated microwave photonic phase shifter with full tunable phase shifting range (>360°) and RF power equalization. *Opt. Express* **2019**, *27*, 14798−14808.
(30) Dong, J.; Zheng, A.; Zhang, Y.; Xia, J.; Tan, S.; Yang, T.; Zhang, X. Photonic Hilbert transformer employing on-chip photonic crystal nanocavity. *J. Lightwave Technol.* **2014**, *32*, 3704−3709.
(31) Nguyen, T. G.; Shoeiby, M.; Chu, S. T.; Little, B. E.; Morandotti, R.; Mitchell, A.; Moss, D. J. Integrated frequency comb source based Hilbert transformer for wideband microwave photonic phase analysis. *Opt. Express* **2015**, *23*, 22087−22097.

https://doi.org/10.1021/acsphotonics.1c00745
ACS Photonics XXXX, XXX, XXX−XXX